



# Adsorption of Reactive Black 5 Dye from Aqueous Solutions by Carbon Nanotubes and its Electrochemical Regeneration Process

Nezamaddin Mengelizadeh<sup>1,\*</sup> and Hamidreza Pourzamani<sup>2</sup>

<sup>1</sup>Department of Environmental Health Engineering, Research Center of Health, Safety and Environment, Faculty of Evaz Health, Larestan University of Medical Sciences, Larestan, Iran

<sup>2</sup>Department of Environmental Health Engineering, School of Health, Isfahan University of Medical Sciences, Isfahan, Iran

\*Corresponding author: Department of Environmental Health Engineering, Larestan University of Medical Sciences, Larestan, Iran. Tel: +98-9392312472, Email: nezam\_m2008@yahoo.com

Received 2020 March 09; Revised 2020 July 30; Accepted 2020 August 11.

## Abstract

Removal of Reactive Black 5 (RB5) dye from aqueous solutions was investigated by adsorption onto Multi-walled Carbon Nanotubes (MWCNTs) and Single-walled Carbon Nanotubes (SWCNTs). A Taguchi orthogonal design including pH, initial RB5 concentration, contact time, and CNTs dose, was used in 16 experiments. The results showed that all four factors were statistically significant, and the optimum conditions for both adsorbents were as follows: pH of 3, adsorbent dose of 1000 mg/L, RB5 concentrations of 25 mg/L, and contact time of 60 min. An equilibrium study by Isotherm Fitting Tool (ISOFIT) software showed that Langmuir isotherm provided the best fit for RB5 adsorption by CNTs. The maximum predicted adsorption capacities for the dye were obtained as 231.84 and 829.20 mg/g by MWCNTs and SWCNTs, respectively. The results also indicated that the adsorption capacity of SWCNTs was about 1.21 folds higher than that of MWCNTs. Studies of electrochemical regeneration were conducted, and the results demonstrated that RB5-loaded MWCNTs and SWCNTs could be regenerated (86.5% and 77.3%, respectively) using the electrochemical process. Adsorbent regeneration was mostly due to the degradation of the dye by the attack of active species such as chlorate, H<sub>2</sub>O<sub>2</sub>, and <sup>•</sup>OH, which were generated by the electrochemical oxidation process with Ti/RuO<sub>2</sub>-IrO<sub>2</sub>-TiO<sub>2</sub> anodes. The results of Gas Chromatography-Mass Spectrometry (GC-MS) analysis showed that acetic acid, 3-chlorobenzenesulfonamide, and 1,2-benzenedicarboxylic acid were produced after adsorbent regeneration by the electrochemical process in the solution of regeneration. The adsorption and regeneration cycles showed that the electrochemical process with Ti/RuO<sub>2</sub>-IrO<sub>2</sub>-TiO<sub>2</sub> and graphite is a good alternative method for the regeneration of CNTs and simultaneous degradation of the dye.

**Keywords:** Reactive Black 5, Adsorption Kinetic, Adsorption Isotherm, ISOFIT Software, Electrochemical Regeneration

## 1. Background

The textile industries use dyes for coloring their final products, and as a result, produce large amounts of organic matter and color-containing effluents (1, 2). The presence of these substances with complex aromatic structures can adversely affect the aqueous environment by reducing photosynthesis activity (1-4). Moreover, most of these aromatic compounds can cause skin irritation and respiratory problems and increase cancer and cell mutation risks in humans (5-7). Therefore, effluents containing dyes require efficient treatment before being discharged into the environment (1). Various methods such as oxidation, adsorption, coagulation, photochemical degradation, and membrane separation are used for the removal of dyes from aqueous solutions (8, 9). Among the mentioned techniques, adsorption has been considered the most attrac-

tive technology due to high efficiency, simplicity, and low cost (10-12). It is a method that transfers contaminants from the liquid phase to a solid phase and, therefore, reduces the bioavailability of stable and aromatic species to living organisms (13). In this method, different adsorbents such as powdered activated carbon (14), chitosan (15), CNTs (1), bamboo activated carbon (16), fly ash (17, 18), chitin (19), zeolite (20), peanut hull (21), carbon nanotubes (12), and Fe<sub>3</sub>O<sub>4</sub>/chitosan (22) have been used for the adsorption of reactive dyes in aqueous environments. Among them, carbon nanotubes have been suggested for the successful removal of different types of pollutants from aqueous solutions because CNTs have favorable physicochemical features such as stability, large specific surface area, high selectivity, hollow and layered structures, and small size (5, 6, 23). Moreover, their functional groups and hydrophobic

surfaces show strong interactions with inorganic and organic compounds (24).

Nonetheless, adsorbents including activated carbon and CNTs are relatively expensive and readily saturated; thus, it is essential to regenerate and reuse them for the treatment of aqueous solutions. Commonly, adsorbents are regenerated by chemical, thermal, and wet air oxidation methods, with serious drawbacks including high cost, expensive equipment, decreasing adsorption capacity, and high energy consumption (25). Recently, adsorbent regeneration by the electrochemical process has been reported as an effective method because of minimal adsorbent losses, 80-95% regeneration efficiencies, and degradation of contaminants desorbed from the adsorbent via oxidation at the anode surface (26, 27). In the process of electrochemical regeneration, pollutants are desorbed from the adsorbent surface by the electro-desorption mechanism and then degraded by electrochemical oxidation (25). Many active species such as hydroxyl radicals, hydrogen peroxide, and HClO contribute to direct or indirect electrochemical oxidation of pollutants (25, 28). Wu et al. treated p-nitrophenol by the electrochemical-adsorption process and found that the electrochemical regeneration was affected by current density, airflow, and the production rate of reactive species (28). Zhou and Lei, by studying the electrochemical regeneration of activated carbon containing p-nitrophenol, reported that the degradation of contaminant molecules on the adsorbent could occur by the attack of free radicals produced by electro-oxidation (26).

It has been reported that the efficiency of electrochemical oxidation is mainly dependent on the electrode material, which is basically divided into active and non-active electrodes. It was also reported that non-active electrodes, such as lead dioxide (PbO<sub>2</sub>) have better efficiency for the destruction of pollutants than have active electrodes such as platinum (Pt) (26). Recently, this type of electrodes has shown a loss of activity due to surface fouling or limited service life (25). To overcome these problems, electrodes with high lifetime and catalytic activity such as Ti/Sb-SnO<sub>2</sub> (29), Ti/Co/SnO<sub>2</sub>-Sb<sub>2</sub>O<sub>5</sub> (30), boron-doped diamond (31), Ti/Pt/PbO<sub>2</sub>, and Si/BDD (32) electrodes have been proposed. Compared to these electrodes, Ti/RuO<sub>2</sub>-IrO<sub>2</sub>-TiO<sub>2</sub> has special characteristics such as large specific surface areas, high mass transfer, rapid production of oxidants, and long-term durability (33-37). However, less attention has been paid to Ti/RuO<sub>2</sub>-IrO<sub>2</sub>-TiO<sub>2</sub> as the anode electrode for the electrochemical regeneration of adsorbents.

## 2. Objectives

The objective of this research was to understand the equilibrium adsorption of RB5 dye on MWCNTs and SWCNTs by investigating the influence of different experimental parameters such as pH, adsorbent dose, initial dye concentration, and contact time. In addition, the regeneration performance of RB5-loaded CNTs was investigated by the electrochemical process with Ti/RuO<sub>2</sub>-IrO<sub>2</sub>-TiO<sub>2</sub> and graphite felt electrodes under various electrolytes and concentrations. In this study, the intermediate products produced from adsorbent regeneration by the electrochemical process were investigated for the first time.

## 3. Methods

### 3.1. Chemicals and Reagents

Textile dye Reactive Black 5 (RB5; CAS Number 17095-24-8; C<sub>26</sub>H<sub>21</sub>N<sub>5</sub>Na<sub>4</sub>O<sub>19</sub>S<sub>6</sub>; 991.82 g/mol; λ<sub>max</sub> = 597 nm) with a purity of ≥ 50% was supplied by Sigma Aldrich (USA). A stock solution was prepared by dissolving the RB5 dye in deionized water to prepare the concentration of 1000 mg/L. Working solutions were prepared by diluting the stock solution of the RB5 dye to the required concentrations (25-200 mg/L). The MWCNTs and SWCNTs with a specific surface area of >100 m<sup>2</sup>/g and an average pore diameter of 1-20 nm were purchased from US research nanomaterials, Inc., (Houston, USA) and used as adsorbents in the study.

### 3.2. Adsorption Experiments

Various experiments were carried out to evaluate the effective parameters in runs designed by the Design of Experiments (DOE) software (Design Expert 7 Stat-Ease, Inc., USA). All of the experiments were conducted in 250 mL glass flasks. In each experiment, a varied amount of CNTs (0-1000 mg/L) was added to 100 mL of dye solution, with the initial concentration of 25-100 mg/L. After preparing each batch system, the flasks were placed on a shaker (Orbital Shaker Model KS260B, IKA Company, Germany) and stirred at 250 rpm at room temperature for 15-60 min. Then, samples were filtered by 0.45 μm polytetrafluoroethylene (PTFE) filters to remove CNT particles. Finally, the residual RB5 concentrations were analyzed. Before and after each experiment, the RB5 concentration was determined using a UV-Vis spectrophotometer at a wavelength of 600 nm. All of the experiments were repeated three times, and only the mean values were reported.

The pH of the solution was measured at the input (pH<sub>in</sub>) and output (pH<sub>out</sub>) in each experiment. The pH<sub>in</sub>

was adjusted using 0.01 M HCl and NaOH and determined by a pH meter (CyberscanpH1500, Thermo Fisher Scientific Inc., Netherlands). The amount of adsorbed RB5 on CNTs ( $q_e$ , mg/g) and removal percentage (R%) were calculated as follows:

$$q_e = \frac{C_0 - C_e}{m} \times V \quad (1)$$

$$\%R = \frac{C_0 - C_e}{C_0} \times 100 \quad (2)$$

Where  $C_0$  and  $C_e$  (mg/L) are the RB5 concentrations at the input and output in each run,  $V$  (L) is the solution volume, and  $m$  (g) is the mass of CNTs.

### 3.3. Analysis of Data

To assess the individual effects of pH, CNTs dosage, RB5 initial concentrations, and contact time on the removal of RB5 and optimize the process condition, DOE software was used. The Taguchi orthogonal plan was applied by four factors at four levels (Appendix 1 in Supplementary File). The matrix involved 16 runs and each run was conducted in triplicate.

An isotherm study was carried out for the RB5 adsorption by CNTs in the optimum condition with the initial concentration of 25–200 mg/L, CNTs dose of 1000 mg/L, contact time of 60 min, and pH of 3. The fit isotherm parameters to experimental data were estimated by the Isotherm Fitting Tool (ISOFIT) software. This software is an analysis program that fits isotherm parameters to experimental data through the minimization of the Weighted Sum of Squared Error (WSSE) of the objective function (38). The ISOFIT supports several isotherms, including 1) Brunauer-Emmett-Teller (BET), 2) Freundlich, 3) Freundlich with Linear Partitioning (F-P), 4) Generalized Langmuir-Freundlich (GLF), 5) Langmuir, 6) Langmuir with Linear Partitioning (L-P), 7) Linear, 8) Polanyi, 9) Polanyi with Linear Partitioning (P-P), and 10) Toth (39).

The pseudo-first-order and pseudo-second-order models are useful for the design and optimization of the RB5 treatment process. Their linear equations are as follows:

$$\ln(q_e - q_t) = \ln q_e - k_1 t \quad (3)$$

$$\frac{t}{q_t} = \frac{1}{k_2 q_e^2} + \frac{t}{q_e} \quad (4)$$

Where  $q_e$  and  $q_t$  are the amounts of RB5 adsorbed (mg/g) at equilibrium and time  $t$  (min), respectively, and  $k_1$  (1/min) and  $k_2$  (g/mg.min) are the rate constants of first-order and second-order adsorption, respectively.

### 3.4. Adsorbent Electrochemical Regeneration

The electrochemical regeneration experiments were conducted in a batch reactor consisting of Ti/RuO<sub>2</sub>-IrO<sub>2</sub>-TiO<sub>2</sub> (anode) and graphite felt (cathode) electrodes. Both anode and cathode had dimensions of 5 cm × 2 mm × 10 cm, and there was a fixed distance of 1 cm between the anode and cathode in those experiments. Before the regeneration process, the RB5 adsorption was performed in the optimum condition, i.e., pH of 3, adsorbent dose of 1000 mg/L, RB5 concentrations of 200 mg/L, and contact time of 120 min. Then, 1 g of used CNTs was put into the electrochemical cell containing 450 mL of electrolyte solution with sodium chloride (NaCl) and sodium sulfate (Na<sub>2</sub>SO<sub>4</sub>). The regeneration experiments were carried out at room temperature. The electrochemical oxidation was stopped after 2 h. After each regeneration, the regenerated CNT was separated from the regeneration solution by PTFE filters to determine its adsorption capacity. In the regeneration process, the influence of different operating parameters was studied by varying one parameter and keeping the other parameters constant (40). To investigate the effect of sodium chloride (NaCl) and sodium sulfate (Na<sub>2</sub>SO<sub>4</sub>) on the CNTs regeneration, different electrolyte concentrations of 0.01, 0.05, and 0.1 M were added into the regeneration solutions. The effect of current density was investigated under the controlled condition at current densities of 10–30 mA/cm<sup>2</sup>.

## 4. Results and Discussion

### 4.1. Effect of Operating Parameters on RB5 Removal

Appendix 2 in Supplementary File shows the RB5 removal percentage by MWCNTs and SWCNTs and equilibrium amounts of adsorbed RB5 on CNTs ( $q_e$ ) under different pHs, initial RB5 concentrations, contact time, and adsorbent doses. The results showed that more than 94% of RB5 was removed by CNTs in run 13, which is in agreement with other studies (39). Figure 1A indicates that the RB5 removal decreased with increasing initial pH from 3 to 9. Therefore, the maximum dye removal by adsorption onto CNTs was achieved at a pH of 3, which can be attributed to the influence of solution pH on the surface of CNTs and dye functional groups (41). At acidic pH, the sulfonate group ( $-\text{SO}_3^-$ ) is present on the RB5 surface, so it is expected that the strong electrostatic attraction occurred between the CNTs adsorption sites and RB5 anions (42). It has been reported in the Machado et al. (43) study that the  $\text{pH}_{\text{pzc}}$  values of MWCNTs and SWCNTs are 6.85 and 6.73, respectively. Therefore, these nanoparticles at pH 3 (a value lower than

the  $pH_{pzc}$ ) are positively charged. On the other hand, lower adsorption capacity in the alkaline condition is due to the competition between hydroxyl ions ( $OH^-$ ) and negatively charged dye ions for the adsorption sites (42, 44). Yao et al. (45) obtained the same results and showed that the amount of RB5 dye adsorbed decreased from 40 mg/g to 24.8 mg/g as the initial pH increased from 2.3 to 10. Also, Machado et al. (46) showed that the adsorption of reactive blue 4 dye on MWCNTs and SWCNTs adsorbents decreased when the initial pH increased from 2 to 10.

The effects of dye initial concentration on the RB5 removal percentage using MWCNTs and SWCNTs were investigated in the RB5 concentration range of 25 to 100 mg/L (Figure 1B). For both adsorbents, RB5 adsorption decreased by raising the dye initial concentration. This may be due to the limitation of free sites available on CNTs for RB5 adsorption. This finding is supported by a study carried out by Balci and Erkurt (47), who reported that the dye removal efficiencies decreased with increasing RB5 initial concentration. This observation is also in agreement with Shirzad-Siboni et al. study (48). Figure 1C shows that the removal rate sharply increased with increasing contact time from 15 to 45 min and then reached the equilibrium in 60 min. Kabbashi et al. (49) reported that Pb(II) sorption reached the equilibrium in 80 min with an initial concentration of 40 mg/L. Moreover, Pourzamani et al. (50) reported that most benzene adsorption on the composite of MSWCNT nanoparticle occurred in 20 min.

The effects of adsorbent dose in the range of 100–1000 mg/L on the RB5 removal are shown in Figure 1D. As can be seen, the percentage of dye removal increased by increasing CNTs' dose from 34.48% to 71.54% for MWCNTs and from 51.5% to 87.17% for SWCNTs. Also, Figure 1D shows that most RB5 removals happened in 1 g/L of CNTs dose that was selected as the optimum condition of CNTs dose. This can be attributed to increasing adsorbent surface areas and active functional groups (44). This result is in agreement with Wu (12) for the adsorption of reactive dye onto carbon nanotubes.

Thus, the optimum conditions for RB5 adsorption by CNTs were the RB5 concentration of 25 mg/L, pH of 3, CNTs dose of 1000 mg/L, and contact time of 60 min. The RB5 removal rates by the adsorption process in the optimum conditions were 94.5% and 95.30% for MWCNTs and SWCNTs, respectively.

#### 4.2. Statistical Analysis

To obtain the individual and combined effect of four different parameters (pH, initial dye concentration, contact time, and adsorbent dose) on adsorption capacity, data

analysis was done and the results are shown in Appendix 3 in Supplementary File. Equations 5 and 6 represent the empirical formula in terms of the above factors:

$$RB5 \text{ removal by MWCNTs} = 53.67 + 18.05A + 15.52B - 9.76C - 19.19D \quad (5)$$

$$RB5 \text{ removal by SWCNTs} = 51.72 + 18.78A + 13.07B - 9.91C - 19.00D \quad (6)$$

The sufficiency of the regression model for the explanation of experimental data at a 95% confidence level was evaluated by the Analysis of Variance (ANOVA). The ANOVA includes some statistical factors such as "Prob-> F", F value, lack of fit,  $R^2$ , and adjusted  $R^2$ . From the ANOVA results (Appendix 3), it is found that the model was highly significant, as the P value for the model was  $< 0.0001$  (P-value  $< 0.05$ ). Also, based on Equation 7, the obtained model F-value was 205.91 for SWCNTs and 252.40 for MWCNTs, which indicates that the model is significant for both adsorbents. Moreover, the F value was selected in the range of 100–450 for the RB5 removal percentage, which offers that the terms of the factors are significant. The insignificance of "lack of fit" with P-values of 0.63 and 0.98 (P-value  $> 0.05$ ) showed that the model satisfactorily fitted the data. A comparison between experimental and calculated values of the sorption capacity is shown in Appendix 4 in the Supplementary File. According to this Appendix, all points lay on a straight line and display a good correlation between predicted values and actual values. This close correlation between the experimental and predicted values of RB5 adsorption was also shown by the values of  $R^2$  and adjusted  $R^2$ .

$$F \text{ value} = \frac{\text{Model mean square}}{\text{Appropriate error mean square}} \quad (7)$$

The contribution of all four factors on the predicted response was calculated by the following formula:

$$\% \text{ contribution} = \frac{\text{mean square of each factor}}{\text{sum of mean squares of all factors}} \quad (8)$$

It is clear from Appendix 3 that the most important variable for the RB5 adsorption system is the adsorbent dose. Almost 44.31% and 43.52% of the contributions to the total RB5 removal were from the MWCNTs and SWCNTs dose factors, respectively. The initial pH also had a significant role in RB5 adsorption efficiency, as it contributed to 26.18 and 28.73% of the predicted responses.

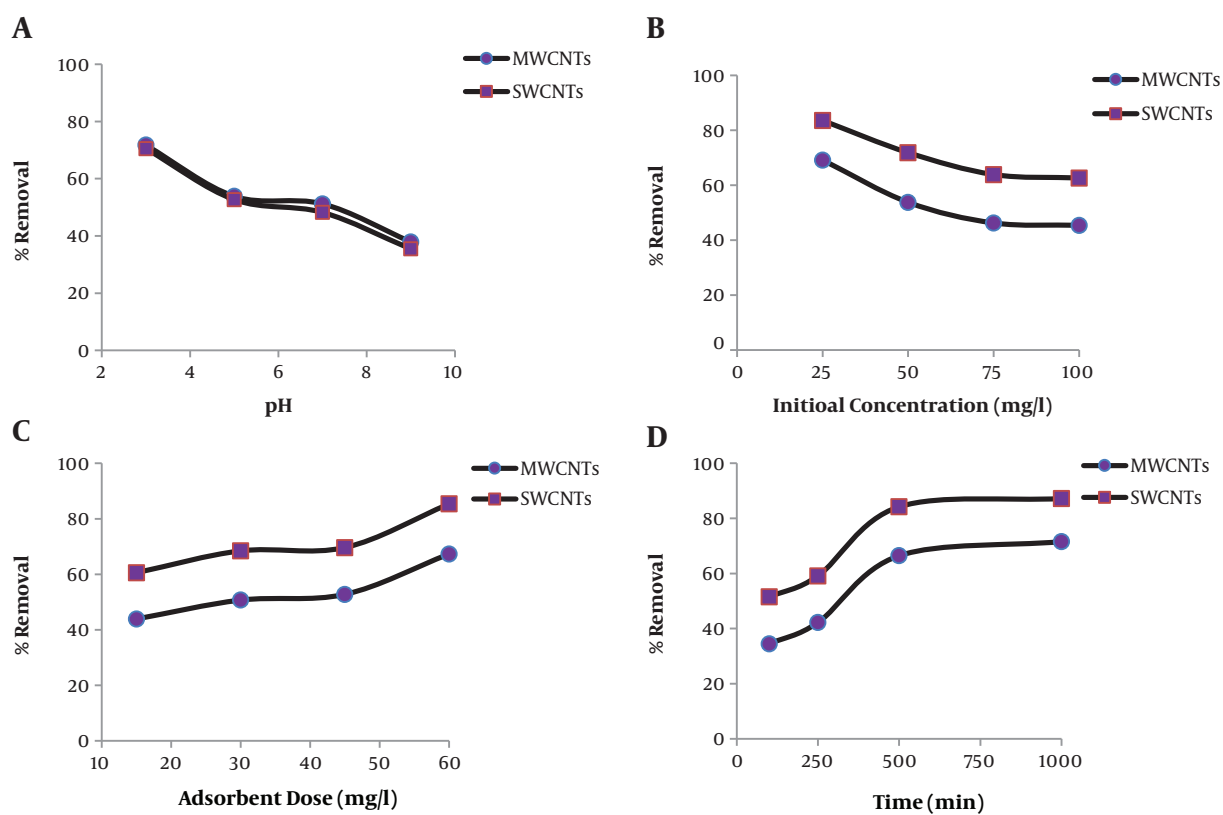


**Figure 1.** Effect of pH (A), RB5 concentration (B), contact time (C), and adsorbent dose (D) on RB5 removal at average levels

#### 4.3. Isotherm Study

The equilibrium data of RB5 adsorption on MWCNTs and SWCNTs were fitted to several well-known isotherm models to evaluate their efficacies. In this study, ISOFIT was selected to assess the adsorption of the RB5 dye at initial concentrations of 25-200 mg/L (25, 50, 75, 100, 150, and 200 mg/L) by MWCNTs and SWCNTs. Appendix 5 and Appendix 6 in Supplementary File summarize some of the diagnostic statistics computed by ISOFIT and reported in the output file for RB5 adsorption by MWCNTs and SWCNTs, respectively. The Akaike Information Criterion (AIC) values indicate that the Langmuir isotherm expression provided the best fit of the sorption data for dye adsorption by both adsorbents. This shows that dye adsorption occurred at specific homogeneous sites on the surface of CNTs. Table 1 contains selected ISOFIT outputs for the Langmuir isotherm for dye adsorption by both adsorbents. Figure 2 shows the plots of the fitted isotherms for dye adsorption by MWCNTs and SWCNTs, along with the observed data points. Bazrafshan et al. (42) studied the adsorption of RB5 from aqueous solutions onto MWCNTs. Their study showed that the Fre-

undlich model could describe the experimental data fairly better than did Langmuir, Temkin, and Dubinin-Radushkevich isotherms. The adsorption process of remazol black B on orange peel studied by Bayrak and Uzgor (51) showed that the adsorption equilibrium data were fitted to the Langmuir isotherm. In another study, ISOFIT was used by Bina et al. (52) to study the adsorption of benzene and toluene by carbon nanotubes. Their results indicated that the Generalized Langmuir-Freundlich (GLF) and Brunauer-Emmett-Teller (BET) isotherms provided the best fit of sorption data for benzene and toluene by CNTs, respectively.

#### 4.4. Absorption Kinetics

To understand the mechanism of adsorption and mass transport processes, the pseudo-first-order and pseudo-second-order models were used to describe the adsorption data. The parameters and correlation coefficients ( $R^2$ ) of kinetic models are listed in Table 2 and Appendix 7. In Table 2, it can be seen that the correlation coefficients ( $R^2$ ) range from 0.9984 to 0.9999, and the calculated  $q_e$  values are in agreement with experimental  $q_e$  values. This indicates that

**Table 1.** Selected ISOFIT Post-Regression Outputs (Langmuir Isotherm)

Parameter or Statistic	ISOFIT Result	
	SWCNTs	MWCNTs
<b>Overall quality of fit</b>		
Weighted sum of squared error	$6.55 \times 10^1$	$3.44 \times 10^2$
Root of mean square error	4.04	9.27
$R_y$	0.99	0.97
<b>Parameter statistics</b>		
$b^* Q_0$	2.25	2.75
b	$2.72 \times 10^{-3}$	$1.19 \times 10^{-2}$
$Q_0$	829.20	231.84
<b>Parameter std. error</b>		
$M^2$	$3.9 \times 10^{-3}$	1.45
Threshold	0.1	0.2
Assessment	Linear	Non-linear
<b>Normality (<math>R_2^N</math>)</b>		
$R_2^N$	0.882	0.94
Assessment	Normal residuals	Normal residuals
<b>Runs test</b>		
Number of runs	3	4
P value	0.65	0.70
Assessment	No correlation	No correlation
<b>Durbin-Watson test (D)</b>		
D	1.5	2.68
P value	0.49	0.49
Assessment	No correlation	No correlation

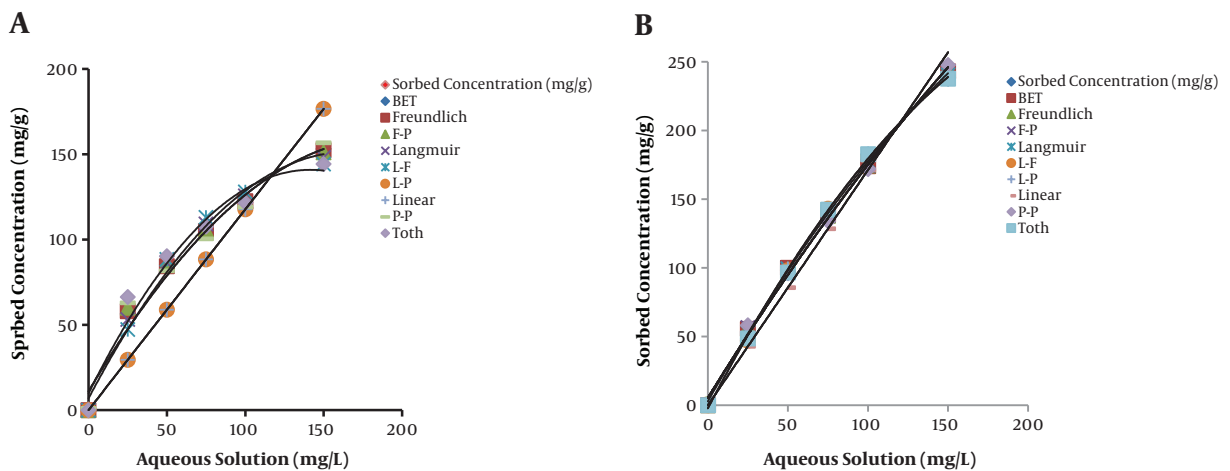


**Figure 2.** Plots of fitted isotherms and observed data for MWCNTs (A) and SWCNTs (B)

the pseudo-second-order model provided the best correlation with experimental data for both adsorbents. Similar results were observed by Wu et al. (12).

The intraparticle diffusion model (Equation 9) is commonly used to investigate the effect of mass transfer stability on the bonding of RB5 molecules in CNTs. In this equation,  $q_t$  (mg/g) is the amount of pollutant absorbed over time,  $k_p$  ( $\text{mg g}^{-1}\text{h}^{1/2}$ ) is the constant rate of intraparticle diffusion, and  $x_i$  (mg/g) is the intercept and boundary layer thickness. The low  $R^2$  value and nonlinear plot (Appendix 7) showed that intraparticle diffusion was not responsible for the adsorption kinetics of RB5 on CNTs,

$$q_t = x_i + k_p t^{0.5} \quad (9)$$

Based on the above results, a comparison was made between different adsorbents in terms of maximum adsorption capacity and the type of adsorption isotherms and kinetics, the results of which are shown in Table 3. As can be seen, the adsorption capacity of CNTs is higher than that of other reported adsorbents, which emphasizes that CNTs with high surface areas can be used as an effective and promising adsorbent.

#### 4.5. Infrared Spectra of Adsorbents

The Fourier Transform-Infrared Spectroscopy (FT-IR) technique was used to identify the functional groups responsible for RB5 adsorption. Figure 3 shows the FT-IR spectra of MWCNTs and SWCNTs before and after the adsorption of RB5 dye. For both adsorbents, intense absorption bands at 3438 and 3427  $\text{cm}^{-1}$  were assigned to O-H bond stretching, before and after the interaction, respectively (6), which indicates that this group played a role in the adsorption of RB5. Also, the peaks at 3000 and 2917  $\text{cm}^{-1}$  represent symmetric stretching of  $\text{CH}_2$  groups, which shows these groups participated in the dye adsorption process. Small bands at 1742  $\text{cm}^{-1}$ , before and after adsorption of the dye by SWCNTs, were assigned to the carbonyl groups of carboxylic acid, respectively. The bands at 1538 and 1483  $\text{cm}^{-1}$  presented on SWCNTs that were assigned to the aromatic ring modes. In addition, strong bands ranging from 900 to 1200  $\text{cm}^{-1}$  before and after adsorption confirmed the presence of the C-O bond. Based on the FT-IR bands, it can be concluded that the adsorption of RB5 dye on CNTs occurred mostly on the groups of hydroxyl (-OH), carboxyl (-COOH), and aromatic rings (6).

Based on the results of FT-IR spectra before and after adsorption, the adsorption mechanism of RB5 by CNTs was proposed, and its schematic is presented in Figure 4. According to a study by Saxena et al. (53), adsorbents containing the functional groups of hydroxyl (-OH), carboxyl

(-COOH), and carboxylate (-COO-) can remove organic contaminants, especially dyes, through hydrogen bonding and electrostatic interaction. In addition, the  $\pi$ - $\pi$  interaction may occur between organic pollutants and adsorbents containing  $\pi$ -electrons. In a study by Saxena et al. (53), it was reported that reactive dyes and CNTs adsorbents have  $\pi$ -electrons and hence, the  $\pi$ - $\pi$  stacking interactions can occur between the aromatic rings of both reagents. According to the identified groups involved in RB5 adsorption in the present study, these mechanisms can play an important role in the adsorption of dye molecules.

#### 4.6. Electrochemical Regeneration

To study the effect of electrochemical regeneration on CNTs adsorption capacity, a series of tests were done under the influence of various factors in the electrochemical cell. The percentage of regeneration is based on the adsorption capacity of regenerated CNTs ( $q_r$ ) and the calculated adsorption capacity ( $q_{cal}$ ) of fresh CNTs at the same liquid-phase concentration.

$$\text{percentage of regeneration} = \frac{q_r}{q_{cal}} \times 100 \quad (10)$$

The results in Figure 5 demonstrate that sodium chloride solution was better than sodium sulfate in CNTs regeneration. This is principally achieved by the hydroxyl and HClO radicals, which are generated on the surface of the electrodes in the electrochemical process, as follows (25, 26):



Zhou and Li (26) found that the p-nitrophenol oxidation on activated carbon was due to anodic oxidation and indirect oxidation by chlorine. Lei et al. (40) also found that the oxidation of ammonia on zeolites was primarily due to the direct and indirect oxidation of chloride. Moreover, according to the experimental results, the adsorption capacity of CNTs regenerated one time was almost equal to that of unused CNTs (Table 4), proving that the electrochemical oxidation method was effective.

The change in the regeneration efficiency with the change in the NaCl concentration is also shown in Figure 5A and B. As shown in the figure, the regeneration efficiency of CNTs increased with an increase in the concentration of NaCl. The addition of NaCl in the electrolysis system

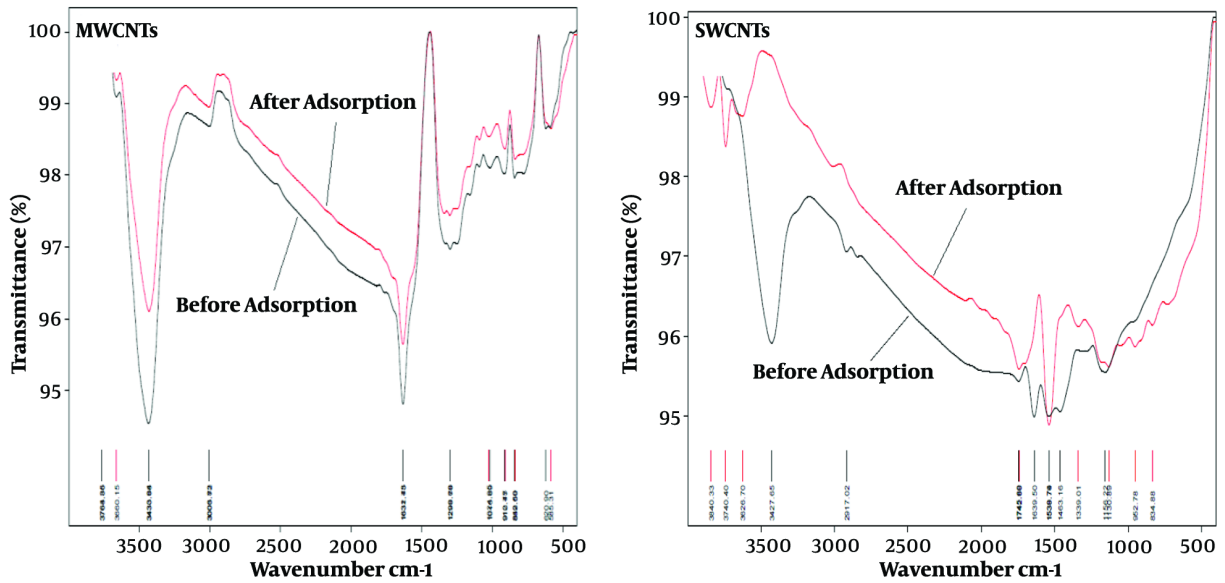


Figure 3. FT-IR spectra of CNTs before and after adsorption of RB5 dye

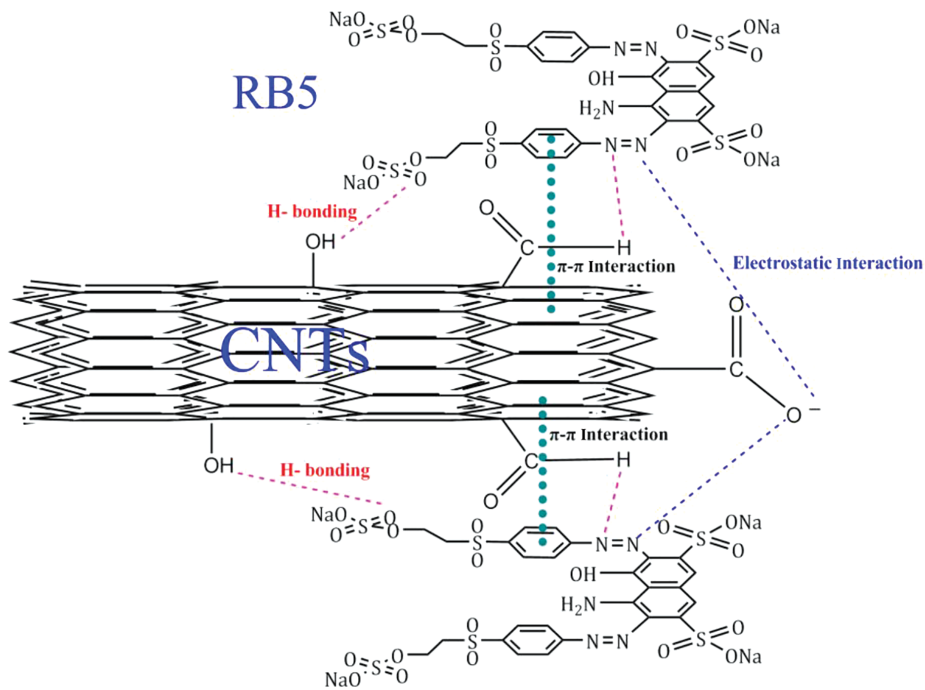


Figure 4. Schematic of the possible mechanism of interaction between RB5 molecules and CNTs

**Table 2.** The First-Order and Second-Order Adsorption Rate Constants, Calculated  $q_e$  ( $q_{e,cal}$ ), and Experimental  $q_e$  Values of RB5 Dye on Adsorbents

Adsorbent	$q_{e,exp}$ (mg/g)	First-Order Kinetic Model			Second-Order Kinetic Model			Intraparticle Diffusion		
		$k_1$ (1/min)	$q_{e,cal}$ (mg/g)	$R^2$	$k_2$ (g/(mg.min)h)	$q_{e,cal}$ (mg/g)	$R^2$	$X_i$	$k_p$	$R^2$
MWCNTs	162.37	0.04	46.05	0.95	0.002	163.93	0.998	125.31	30.66	0.87
SWCNTs	196.75	0.05	22.26	0.90	0.005	200	0.999	180.28	14.39	0.60

**Table 3.** Comparison of Adsorption Capacities of Various Adsorbents for Dyes

Adsorbents	Pollutant Type	$q_{max}$ (mg/g)	Isotherm	Kinetic Model	Sources
SWCNTs	RB5	829.2	Langmuir	Pseudo-second-order	This work
MWCNTs		231.84			
Nanohydroxyapatite	Reactive Blue 19	90.09	Langmuir	Pseudo-second-order	(10)
Chitosan	Remazol black 13	130	Langmuir	Intraparticle diffusion	(15)
Active carbon	RB5	198	Langmuir	Pseudo-second-order	(16)
Bone char		160	Freundlich	Pseudo-first-order	(16)
Fly ash	RB5	4.38	Langmuir	Pseudo-second-order	(18)
	Reactive Yellow 176	3.65	Langmuir		
Peanut hull	RB5	50	Langmuir	Pseudo-second-order	(21)

**Table 4.** Efficiency of CNTs Regeneration

Time	Adsorbent	Control	1	2
Adsorption capacity (mg/g)	SWCNTs	196.75	173.16	131.40
	MWCNTs	162.36	121.69	76.98

resulted in the production of chlorine and hypochlorite ions (Equations 12–14), as well as the increase in conductivity of the electrolyte. This finding is supported by a study carried out by Zhang (54), who reported that the regeneration efficiencies increased with increasing electrolyte concentration.

Current density is one of the most important factors in the electrochemical regeneration process. The effect of current density on the regeneration of CNTs is shown in Figure 5C. For both adsorbents, the regeneration efficiency increased with increasing current density. This is due to the increased oxygen evolution and enhanced chlorine/hypochlorite formation rates (40). Similar results were reported in the electrochemical regeneration of activated carbon loaded with p-nitrophenol (26) and granular activated carbon loaded with phenol (27). Moreover, Czarnetzki and Janssen (55) reported that increased oxygen evolution and chlorate formation rates occurred by increasing current density in the electrolysis process.

Regeneration time is also another key parameter affecting regeneration efficiency and energy consumption (25). Figure 5D shows the effect of regeneration time on electrochemical regeneration. As seen, the regeneration ef-

iciency increases with increasing the time up to 120 min and then stayed almost constant. This can be simply attributed to the increase in oxygen evolution and oxidant formation rates. Zhang (54) found that the regeneration rate of activated carbon increased quickly with contact time and then slowly reached the equilibrium in 5 h.

To further understand the effect of the electrochemical oxidation process on adsorbent regeneration and dye degradation, GC-MS analysis was carried out for identifying the intermediate products in the regeneration solution. According to Figure 6, some organic acid compounds, such as acetic acid and benzocarboxylic acid, were generated in the system.

## 5. Conclusions

The optimum condition was investigated to identify the highest capacity of carbon nanotubes for RB5 dye adsorption. Four controlling factors including pH, dye concentration, contact time, and CNTs dose at four different levels were applied. According to the results, the optimal condition occurred at a pH of 3, RB5 concentration of 25 mg/L, adsorbent dose of 1000 mg/L, and contact time of 60 min. The best fit kinetic and isotherm models were

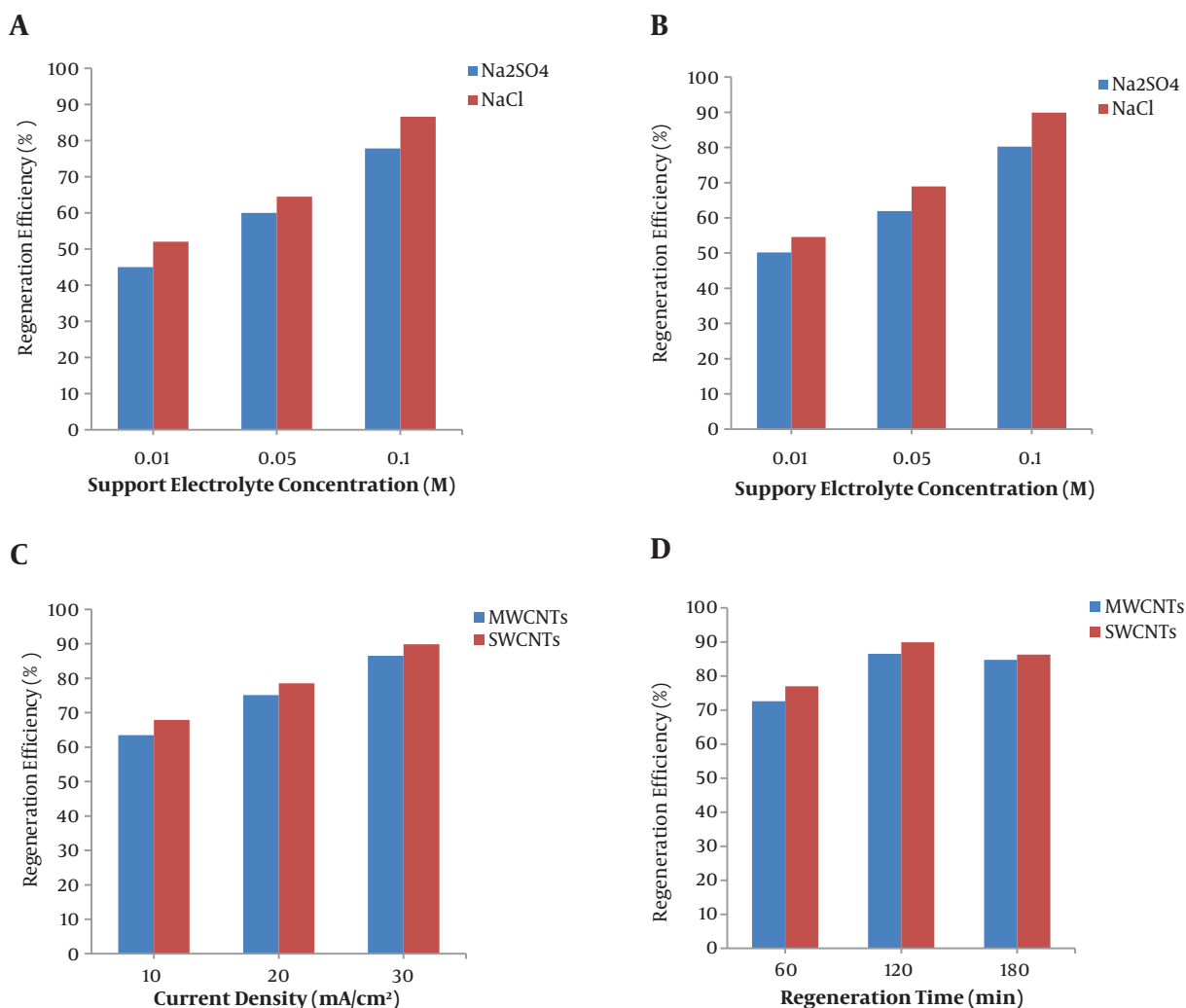


**Figure 5.** Regeneration efficiency of MWCNTs and SWCNTs in different electrolyte concentrations, current density, and time (total experimental conditions: initial pH=3, CNTs = 1 g/L, current density= 30 mA/cm<sup>2</sup>, NaCl concentration=0.1 M, and regeneration time = 120 min)

determined to be the pseudo-second-order kinetic model and Langmuir isotherm model, respectively. The high  $F$ ,  $R^2$ , and  $R^2$  adjusted values showed the quadratic polynomial model was suitable for modeling the adsorption process. The regeneration study was conducted using the electrochemical process, and it was observed that > 70% dye could be desorbed from the CNTs surface, and then degraded by electrochemical oxidation. The results indicated that CNTs could be used as an efficient adsorbent for the removal of reactive black 5 dye from aqueous solutions. Also, the combination of electrochemical and adsorption processes would be an efficient process for dye treatment and regeneration of adsorbents used.

### Supplementary Material

Supplementary material(s) is available [here](#) [To read supplementary materials, please refer to the journal website and open PDF/HTML].

### Acknowledgments

We are grateful for the financial support provided by the Student Research Committee of Isfahan University of Medical Sciences.

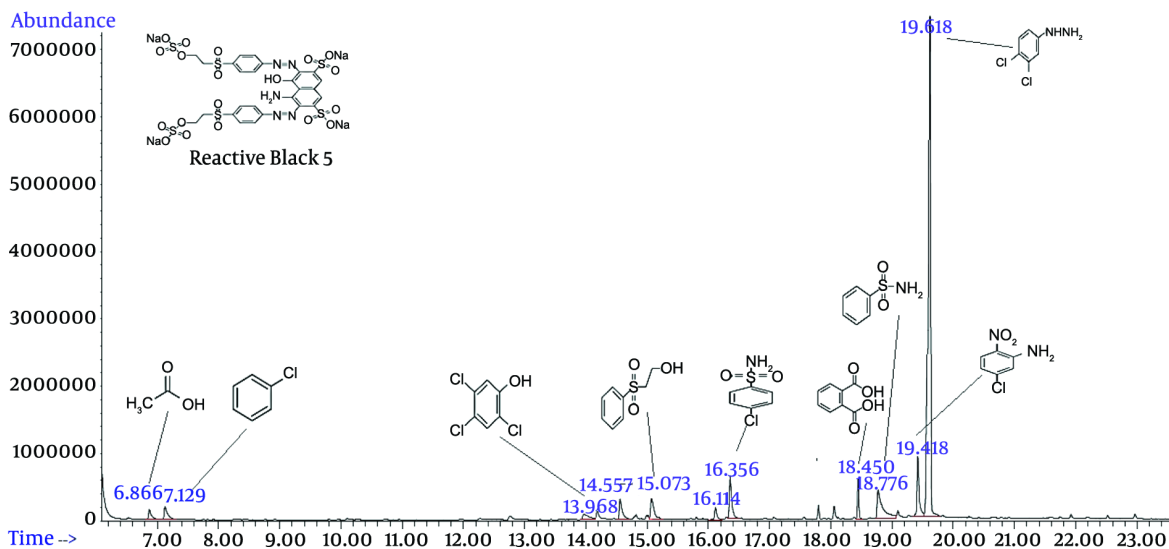


Figure 6. GC-MS chromatograms of samples taken of electrochemical regeneration of adsorbents

## Footnotes

**Authors' Contribution:** Hamidreza Pourzamani: Analysis and interpretation of data, study concept, and design, and study supervision. Nezamaddin Mengelizadeh: Writing the manuscript, analysis and interpretation of data, and statistical analysis.

**Conflict of Interests:** There were no conflicts of interest to declare.

**Ethical Approval:** Ethical approval was not required because it was a wastewater treatment and laboratory study.

**Funding/Support:** Isfahan University of Medical Sciences funded the study.

## References

- Prola LD, Machado FM, Bergmann CP, de Souza FE, Gally CR, Lima EC, et al. Adsorption of Direct Blue 53 dye from aqueous solutions by multi-walled carbon nanotubes and activated carbon. *J Environ Manage.* 2013;**130**:166-75. doi: [10.1016/j.jenvman.2013.09.003](https://doi.org/10.1016/j.jenvman.2013.09.003). [PubMed: [24076517](https://pubmed.ncbi.nlm.nih.gov/24076517/)].
- Madrakian T, Afkhami A, Ahmadi M, Bagheri H. Removal of some cationic dyes from aqueous solutions using magnetic-modified multi-walled carbon nanotubes. *J Hazard Mater.* 2011;**196**:109-14. doi: [10.1016/j.jhazmat.2011.08.078](https://doi.org/10.1016/j.jhazmat.2011.08.078). [PubMed: [21930344](https://pubmed.ncbi.nlm.nih.gov/21930344/)].
- Yao Y, Xu F, Chen M, Xu Z, Zhu Z. Adsorption behavior of methylene blue on carbon nanotubes. *Bioresour Technol.* 2010;**101**(9):3040-6. doi: [10.1016/j.biortech.2009.12.042](https://doi.org/10.1016/j.biortech.2009.12.042). [PubMed: [20060712](https://pubmed.ncbi.nlm.nih.gov/20060712/)].
- Gong JL, Wang B, Zeng GM, Yang CP, Niu CG, Niu QY, et al. Removal of cationic dyes from aqueous solution using magnetic multi-wall carbon nanotube nanocomposite as adsorbent. *J Hazard Mater.* 2009;**164**(2-3):1517-22. doi: [10.1016/j.jhazmat.2008.09.072](https://doi.org/10.1016/j.jhazmat.2008.09.072). [PubMed: [18977077](https://pubmed.ncbi.nlm.nih.gov/18977077/)].
- Tan KB, Vakili M, Horri BA, Poh PE, Abdullah AZ, Salamatinia B. Adsorption of dyes by nanomaterials: Recent developments and adsorption mechanisms. *Separation and Purification Technology.* 2015;**150**:229-42. doi: [10.1016/j.seppur.2015.07.009](https://doi.org/10.1016/j.seppur.2015.07.009).
- Machado FM, Bergmann CP, Fernandes TH, Lima EC, Royer B, Calvete T, et al. Adsorption of Reactive Red M-2BE dye from water solutions by multi-walled carbon nanotubes and activated carbon. *J Hazard Mater.* 2011;**192**(3):1122-31. doi: [10.1016/j.jhazmat.2011.06.020](https://doi.org/10.1016/j.jhazmat.2011.06.020). [PubMed: [21724329](https://pubmed.ncbi.nlm.nih.gov/21724329/)].
- Cardoso NF, Lima EC, Royer B, Bach MV, Dotto GL, Pinto LA, et al. Comparison of Spirulina platensis microalgae and commercial activated carbon as adsorbents for the removal of Reactive Red 120 dye from aqueous effluents. *J Hazard Mater.* 2012;**241-242**:146-53. doi: [10.1016/j.jhazmat.2012.09.026](https://doi.org/10.1016/j.jhazmat.2012.09.026). [PubMed: [23040660](https://pubmed.ncbi.nlm.nih.gov/23040660/)].
- Yagub MT, Sen TK, Afroze S, Ang HM. Dye and its removal from aqueous solution by adsorption: a review. *Adv Colloid Interface Sci.* 2014;**209**:172-84. doi: [10.1016/j.cis.2014.04.002](https://doi.org/10.1016/j.cis.2014.04.002). [PubMed: [24780401](https://pubmed.ncbi.nlm.nih.gov/24780401/)].
- Zhao D, Zhang W, Chen C, Wang X. Adsorption of Methyl Orange Dye Onto Multiwalled Carbon Nanotubes. *Procedia Environmental Sciences.* 2013;**18**:890-5. doi: [10.1016/j.proenv.2013.04.120](https://doi.org/10.1016/j.proenv.2013.04.120).
- Ciobanu G, Barna S, Harja M. Kinetic and equilibrium studies on adsorption of Reactive Blue 19 dye from aqueous solutions by nanohydroxyapatite adsorbent. *Archives of Environmental Protection.* 2016;**42**(2):3-11. doi: [10.1515/aep-2016-0014](https://doi.org/10.1515/aep-2016-0014).
- Kuo CY, Wu CH, Wu JY. Adsorption of direct dyes from aqueous solutions by carbon nanotubes: determination of equilibrium, kinetics and thermodynamics parameters. *J Colloid Interface Sci.* 2008;**327**(2):308-15. doi: [10.1016/j.jcis.2008.08.038](https://doi.org/10.1016/j.jcis.2008.08.038). [PubMed: [18786679](https://pubmed.ncbi.nlm.nih.gov/18786679/)].
- Wu CH. Adsorption of reactive dye onto carbon nanotubes: equilibrium, kinetics and thermodynamics. *J Hazard Mater.* 2007;**144**(1-2):93-100. doi: [10.1016/j.jhazmat.2006.09.083](https://doi.org/10.1016/j.jhazmat.2006.09.083). [PubMed: [17081687](https://pubmed.ncbi.nlm.nih.gov/17081687/)].

13. Ribas MC, Adebayo MA, Prola LD, Lima EC, Cataluña R, Feris LA, et al. Comparison of a homemade cocoa shell activated carbon with commercial activated carbon for the removal of reactive violet 5 dye from aqueous solutions. *Chemical Engineering Journal*. 2014;**248**:315–26. doi: [10.1016/j.cej.2014.03.054](https://doi.org/10.1016/j.cej.2014.03.054).
14. Eren Z, Acar FN. Adsorption of Reactive Black 5 from an aqueous solution: equilibrium and kinetic studies. *Desalination*. 2006;**194**(1-3):1–10. doi: [10.1016/j.desal.2005.10.022](https://doi.org/10.1016/j.desal.2005.10.022).
15. Annadurai G, Ling LY, Lee JF. Adsorption of reactive dye from an aqueous solution by chitosan: isotherm, kinetic and thermodynamic analysis. *J Hazard Mater*. 2008;**152**(1):337–46. doi: [10.1016/j.jhazmat.2007.07.002](https://doi.org/10.1016/j.jhazmat.2007.07.002). [PubMed: 17686579].
16. Ip AW, Barford JP, McKay G. A comparative study on the kinetics and mechanisms of removal of Reactive Black 5 by adsorption onto activated carbons and bone char. *Chemical Engineering Journal*. 2010;**157**(2-3):434–42. doi: [10.1016/j.cej.2009.12.003](https://doi.org/10.1016/j.cej.2009.12.003).
17. Dizge N, Aydinler C, Demirbas E, Kobya M, Kara S. Adsorption of reactive dyes from aqueous solutions by fly ash: kinetic and equilibrium studies. *J Hazard Mater*. 2008;**150**(3):737–46. doi: [10.1016/j.jhazmat.2007.05.027](https://doi.org/10.1016/j.jhazmat.2007.05.027). [PubMed: 17574338].
18. Pengthamkeerati P, Satapanajaru T, Singchan O. Sorption of reactive dye from aqueous solution on biomass fly ash. *J Hazard Mater*. 2008;**153**(3):1149–56. doi: [10.1016/j.jhazmat.2007.09.074](https://doi.org/10.1016/j.jhazmat.2007.09.074). [PubMed: 17981394].
19. Akkaya G, Uzun İ, Güzel F. Kinetics of the adsorption of reactive dyes by chitin. *Dyes and Pigments*. 2007;**73**(2):168–77. doi: [10.1016/j.dyepig.2005.11.005](https://doi.org/10.1016/j.dyepig.2005.11.005).
20. Armağan B, Turan M, Elik MS. Equilibrium studies on the adsorption of reactive azo dyes into zeolite. *Desalination*. 2004;**170**(1):33–9. doi: [10.1016/j.desal.2004.02.091](https://doi.org/10.1016/j.desal.2004.02.091).
21. Tanyildizi M. Modeling of adsorption isotherms and kinetics of reactive dye from aqueous solution by peanut hull. *Chemical Engineering Journal*. 2011;**168**(3):1234–40. doi: [10.1016/j.cej.2011.02.021](https://doi.org/10.1016/j.cej.2011.02.021).
22. Cao C, Xiao L, Chen C, Shi X, Cao Q, Gao L. In situ preparation of magnetic Fe<sub>3</sub>O<sub>4</sub>/chitosan nanoparticles via a novel reduction-precipitation method and their application in adsorption of reactive azo dye. *Powder Technology*. 2014;**260**:90–7. doi: [10.1016/j.powtec.2014.03.025](https://doi.org/10.1016/j.powtec.2014.03.025).
23. Upadhyayula VK, Deng S, Mitchell MC, Smith GB. Application of carbon nanotube technology for removal of contaminants in drinking water: a review. *Sci Total Environ*. 2009;**408**(1):1–13. doi: [10.1016/j.scitotenv.2009.09.027](https://doi.org/10.1016/j.scitotenv.2009.09.027). [PubMed: 19819525].
24. Ren X, Chen C, Nagatsu M, Wang X. Carbon nanotubes as adsorbents in environmental pollution management: A review. *Chemical Engineering Journal*. 2011;**170**(2-3):395–410. doi: [10.1016/j.cej.2010.08.045](https://doi.org/10.1016/j.cej.2010.08.045).
25. Zhang C, Jiang Y, Li Y, Hu Z, Zhou L, Zhou M. Three-dimensional electrochemical process for wastewater treatment: A general review. *Chemical Engineering Journal*. 2013;**228**:455–67. doi: [10.1016/j.cej.2013.05.033](https://doi.org/10.1016/j.cej.2013.05.033).
26. Zhou MH, Lei LC. Electrochemical regeneration of activated carbon loaded with p-nitrophenol in a fluidized electrochemical reactor. *Electrochimica Acta*. 2006;**51**(21):4489–96. doi: [10.1016/j.electacta.2005.12.028](https://doi.org/10.1016/j.electacta.2005.12.028).
27. Narbaitz RM, Karimi-Jashni A. Electrochemical regeneration of granular activated carbons loaded with phenol and natural organic matter. *Environ Technol*. 2009;**30**(1):27–36. doi: [10.1080/09593330802422803](https://doi.org/10.1080/09593330802422803). [PubMed: 19213463].
28. Wu Z, Cong Y, Zhou M, Tan T. -Nitrophenol abatement by the combination of electrocatalysis and activated carbon. *Chemical Engineering Journal*. 2005;**106**(1):83–90. doi: [10.1016/j.cej.2004.10.009](https://doi.org/10.1016/j.cej.2004.10.009).
29. Fockedeey E, Van Lierde A. Coupling of anodic and cathodic reactions for phenol electro-oxidation using three-dimensional electrodes. *Water Research*. 2002;**36**(16):4169–75. doi: [10.1016/S0043-1354\(02\)00103-3](https://doi.org/10.1016/S0043-1354(02)00103-3).
30. Wang B, Kong W, Ma H. Electrochemical treatment of paper mill wastewater using three-dimensional electrodes with Ti/Co/SnO<sub>2</sub>-Sb<sub>2</sub>O<sub>5</sub> anode. *J Hazard Mater*. 2007;**146**(1-2):295–301. doi: [10.1016/j.jhazmat.2006.12.031](https://doi.org/10.1016/j.jhazmat.2006.12.031). [PubMed: 17222510].
31. Zhu X, Ni J, Xing X, Li H, Jiang Y. Synergies between electrochemical oxidation and activated carbon adsorption in three-dimensional boron-doped diamond anode system. *Electrochimica Acta*. 2011;**56**(3):1270–4. doi: [10.1016/j.electacta.2010.10.073](https://doi.org/10.1016/j.electacta.2010.10.073).
32. Ciriaco L, Anjo C, Correia J, Pacheco MJ, Lopes A. Electrochemical degradation of Ibuprofen on Ti/Pt/PbO<sub>2</sub> and Si/BDD electrodes. *Electrochimica Acta*. 2009;**54**(5):1464–72. doi: [10.1016/j.electacta.2008.09.022](https://doi.org/10.1016/j.electacta.2008.09.022).
33. Chen J, Shi H, Lu J. Electrochemical treatment of ammonia in wastewater by RuO<sub>2</sub>-IrO<sub>2</sub>-TiO<sub>2</sub>/Ti electrodes. *Journal of Applied Electrochemistry*. 2007;**37**(10):1137–44. doi: [10.1007/s10800-007-9373-6](https://doi.org/10.1007/s10800-007-9373-6).
34. Wu J, Zhang H, Oturan N, Wang Y, Chen L, Oturan MA. Application of response surface methodology to the removal of the antibiotic tetracycline by electrochemical process using carbon-felt cathode and DSA (Ti/RuO<sub>2</sub>-IrO<sub>2</sub>) anode. *Chemosphere*. 2012;**87**(6):614–20. doi: [10.1016/j.chemosphere.2012.01.036](https://doi.org/10.1016/j.chemosphere.2012.01.036). [PubMed: 22342334].
35. Daghrir R, Drogui P, Delegan N, El Khakani MA. Electrochemical degradation of chlortetracycline using N-doped Ti/TiO<sub>2</sub> photoanode under sunlight irradiations. *Water Res*. 2013;**47**(17):6801–10. doi: [10.1016/j.watres.2013.09.011](https://doi.org/10.1016/j.watres.2013.09.011). [PubMed: 24075724].
36. Daghrir R, Drogui P, Ka I, El Khakani MA. Photoelectrocatalytic degradation of chlortetracycline using Ti/TiO<sub>2</sub> nanostructured electrodes deposited by means of a Pulsed Laser Deposition process. *J Hazard Mater*. 2012;**199-200**:15–24. doi: [10.1016/j.jhazmat.2011.10.022](https://doi.org/10.1016/j.jhazmat.2011.10.022). [PubMed: 22104083].
37. Kozliak EI, Paca J. Part A. Toxic/hazardous substances and environmental engineering. *Journal of environmental science and health*. 2012;**47**(7):919.
38. Matott L, Rabideau AJ. ISOFIT – A program for fitting sorption isotherms to experimental data. *Environmental Modelling & Software*. 2008;**23**(5):670–6. doi: [10.1016/j.envsoft.2007.08.005](https://doi.org/10.1016/j.envsoft.2007.08.005).
39. Amin MM, Bina B, Majd AMS, Pourzamani H. Benzene removal by nano magnetic particles under continuous condition from aqueous solutions. *Frontiers of Environmental Science & Engineering*. 2013;**8**(3):345–56. doi: [10.1007/s11783-013-0574-4](https://doi.org/10.1007/s11783-013-0574-4).
40. Lei X, Li M, Zhang Z, Feng C, Bai W, Sugiura N. Electrochemical regeneration of zeolites and the removal of ammonia. *J Hazard Mater*. 2009;**169**(1-3):746–50. doi: [10.1016/j.jhazmat.2009.04.012](https://doi.org/10.1016/j.jhazmat.2009.04.012). [PubMed: 1941139].
41. Rao G, Lu C, Su F. Sorption of divalent metal ions from aqueous solution by carbon nanotubes: A review. *Separation and Purification Technology*. 2007;**58**(1):224–31. doi: [10.1016/j.seppur.2006.12.006](https://doi.org/10.1016/j.seppur.2006.12.006).
42. Bazrafshan E, Kord Mostafapour F, Rahdar S, Mahvi AH. Equilibrium and thermodynamics studies for decolorization of Reactive Black 5 (RB5) by adsorption onto MWCNTs. *Desalination and Water Treatment*. 2014;**54**(8):2241–51. doi: [10.1080/19443994.2014.895778](https://doi.org/10.1080/19443994.2014.895778).
43. Machado FM, Carmalin SA, Lima EC, Dias SL, Prola LD, Saucier C, et al. Adsorption of Alizarin Red S Dye by Carbon Nanotubes: An Experimental and Theoretical Investigation. *The Journal of Physical Chemistry C*. 2016;**120**(32):18296–306. doi: [10.1021/acs.jpcc.6b03884](https://doi.org/10.1021/acs.jpcc.6b03884).
44. Toprak F, Armağan B, Cakici A. Systematic approach for the optimal process conditions of Reactive Red 198 adsorption by pistachio nut shell using Taguchi method. *Desalination and Water Treatment*. 2012;**48**(1-3):96–105. doi: [10.1080/19443994.2012.698800](https://doi.org/10.1080/19443994.2012.698800).
45. Yao Y, Bing H, Feifei X, Xiaofeng C. Equilibrium and kinetic studies of methyl orange adsorption on multiwalled carbon nanotubes. *Chemical Engineering Journal*. 2011;**170**(1):82–9. doi: [10.1016/j.cej.2011.03.031](https://doi.org/10.1016/j.cej.2011.03.031).
46. Machado FM, Bergmann CP, Lima EC, Royer B, de Souza FE, Jauris IM, et al. Adsorption of Reactive Blue 4 dye from water solutions by carbon nanotubes: experiment and theory. *Phys Chem Chem Phys*.

- 2012;**14**(31):11139–53. doi: [10.1039/c2cp41475a](https://doi.org/10.1039/c2cp41475a). [PubMed: 22781834].
47. Balci B, Erkurt FE. Adsorption of reactive dye from aqueous solution and synthetic dye bath wastewater by Eucalyptus bark/magnetite composite. *Water Sci Technol*. 2016;**74**(6):1386–97. doi: [10.2166/wst.2016.323](https://doi.org/10.2166/wst.2016.323). [PubMed: 27685968].
48. Shirzad-Siboni M, Jafari SJ, Giahi O, Kim I, Lee S, Yang J. Removal of acid blue 113 and reactive black 5 dye from aqueous solutions by activated red mud. *Journal of Industrial and Engineering Chemistry*. 2014;**20**(4):1432–7. doi: [10.1016/j.jiec.2013.07.028](https://doi.org/10.1016/j.jiec.2013.07.028).
49. Kabbashi NA, Atieh MA, Al-Mamun A, Mirghami ME, Alam MDZ, Yahya N. Kinetic adsorption of application of carbon nanotubes for Pb(II) removal from aqueous solution. *Journal of Environmental Sciences*. 2009;**21**(4):539–44. doi: [10.1016/S1001-0742\(08\)62305-0](https://doi.org/10.1016/S1001-0742(08)62305-0).
50. Pourzamani H, Samani Majd AM, Fadaei S. Benzene removal by hybrid of nanotubes and magnetic nanoparticle from aqueous solution. *Desalination and Water Treatment*. 2015;**57**(40):19038–49. doi: [10.1080/19443994.2015.1098569](https://doi.org/10.1080/19443994.2015.1098569).
51. Bayrak Y, Uzgör R. Removal of Remazol Black B Textile Dye from Aqueous Solution by Adsorption: Equilibrium and Thermodynamic Studies. *Journal of Dispersion Science and Technology*. 2013;**34**(6):828–33. doi: [10.1080/01932691.2012.704749](https://doi.org/10.1080/01932691.2012.704749).
52. Bina B, Amin M, Rashidi A, Pourzamani H. Benzene and Toluene Removal by Carbon Nanotubes from Aqueous Solution. *Archives of Environmental Protection*. 2012;**38**(1). doi: [10.2478/v10265-012-0001-0](https://doi.org/10.2478/v10265-012-0001-0).
53. Saxena R, Saxena M, Lochab A. Recent progress in nanomaterials for adsorptive removal of organic contaminants from wastewater. *ChemistrySelect*. 2020;**5**(1):335–53. doi: [10.1002/slct.201903542](https://doi.org/10.1002/slct.201903542).
54. Zhang H. Regeneration of exhausted activated carbon by electrochemical method. *Chemical Engineering Journal*. 2002;**85**(1):81–5. doi: [10.1016/S1385-8947\(01\)00176-0](https://doi.org/10.1016/S1385-8947(01)00176-0).
55. Czarnetzki LR, Janssen LJJ. Formation of hypochlorite, chlorate and oxygen during NaCl electrolysis from alkaline solutions at an RuO<sub>2</sub>/TiO<sub>2</sub> anode. *Journal of Applied Electrochemistry*. 1992;**22**(4):315–24. doi: [10.1007/bf01092683](https://doi.org/10.1007/bf01092683).